Aerodynamic Theory for Wing with Side Edge Passing Subsonically through a Gust

Rudolph Martinez* and Sheila E. Widnall†
Massachusetts Institute of Technology, Cambridge, Massachusetts

An approximate solution for the unsteady loading near the square-shape tip of a wing passing through an oblique gust is obtained in closed form. The aerodynamic theory developed can be used to predict airloads felt by a helicopter blade experiencing a blade/vortex interaction for high blade tip speed and/or for small vertical blade/vortex separation. Under these conditions one can show that the blade's trailing edge has little influence on the character of the chordwise loading at all spanwise sections; thus, the chord may be allowed to extend to infinity in the downstream direction. Therefore, the model considered here is that of a quarter-infinite flat plate wing with side edge passing subsonically through an oblique gust.

Nomenclature

A	= function defined in Eq. (16)
b	= wing semichord, reference length
c_0	= sound speed
D/Dt	= substantial derivative
E, E^*	= Fresnel integral and its complex conjugate
f	= function in convolution, Eq. (26)
$H_1^{(2)}$	= Hankel function
I	= integral defined in Eq. (24)
k_x	= reduced frequency, or nondimensional chordwise wave number
K	$= k_x M/(1-M^2)$
M	= freestream Mach number
P, p_*	= perturbation pressures
r	= assumed form for three-dimensional upwash, Eqs. (12a) and (14)
$\tilde{r}$	= Fourier transform of r
t	= time
U	= subsonic freestream velocity, or flight speed
v	= assumed form for three-dimensional upwash, Eq. (12b)
$\tilde{v}$	= Fourier transform of v
w_0	= gust amplitude
x, y, z	= chordwise, spanwise, and normal to wing spatial coordinates
Y, Z	$= \sqrt{1-M^2}\, y$, $\sqrt{1-M^2}\, z$, respectively
Φ, ϕ_*	= perturbation velocity potentials
γ	= Euler's constant, 0.577...
λ_{gust}	= gust wavelength
Λ	= wing/gust interaction angle
μ	= frequency parameter $= (k_x/(1-M^2))\,\lvert\tan\Lambda\rvert\,(M^2/\sin^2\Lambda - 1)^{1/2}$
ρ_0	= freestream density

Introduction

THE computation of airloads on a wing of arbitrary geometry in unsteady flow remains a formidable task, even for those cases which allow a linearized analysis. In the present paper we develop an approximate, closed-form lifting-surface theory for the special case of a thin, semi-infinite span wing with a single side edge passing through an oblique sinusoidal gust convected by a subsonic freestream. The model is motivated by the need to determine the unsteady pressure distribution near the tip of a helicopter blade passing over a vortex trailing from another rotor blade. The unsteady loading predicted here will serve as a distribution of acoustic dipoles in future noise calculations.

We limit our analysis to those wing/gust interaction cases for which the gust is of short wavelength in comparison to the wing semichord and/or for which the freestream Mach number is close to 1. Adamczyk,[1] Amiet,[2] and the authors[3] have demonstrated that in such operating regimes a wing's trailing edge has little effect on chordwise pressure distributions, and thus that the loading obtained considering the presence of the leading edge alone satisfies almost automatically the conditions of $\Delta P = 0$ at the trailing-edge position (the Kutta condition) and in the wake. In our analysis we take advantage of this fact and ignore the presence of the wing's trailing edge: the chord is assumed to extend infinitely in the downstream direction from the leading edge, so that the planform's geometry is a quarter-infinite flat plate occupying the region $x>0$, $y>0$ of the x-y plane. Sweep effects are not considered. The side edge ($x>0$, $y=0$) remains always a true side edge aligned with the freestream, never acting as either a leading or a trailing edge.

Furthermore, we consider only those interaction angle Λ/Mach number M combinations which satisfy the condition $\sin\Lambda > M$, a condition which implies physically that unsteady load fronts travel subsonically through the still fluid and which is often met by blade/vortex interactions for single-rotor helicopters. For $\sin\Lambda < M$ (supersonic trace speeds) we expect the acoustic field to be dominated by radiation from sources along the wing's leading edge, with strengths that may be predicted using two-dimensional aerodynamic models by Adamczyk[1] and Amiet,[2] who in their studies neglect the three-dimensional side-edge effects that are the issue of the present paper.

For transonic and supersonic flows, respectively, Landahl[4] and Miles[5] have given exact solutions to the closely related problem of a corner wing undergoing harmonic oscillations. For subsonic flow, we find here that although the gust problem has no exact closed-form solution analogous to theirs, an approximate lifting-surface theory, useful for theoretical noise studies, may be extracted rationally after some analysis. In a paper to follow we apply this aerodynamic result to calculate the strength of acoustic sources near the tip of a helicopter blade of finite length passing over a potential vortex, and the resulting acoustic field. The sinusoidal gust in the present model is used as a Fourier component of the

Received April 16, 1982; revision received Sept. 30, 1982.

*Post-Doctoral Research Associate. Currently with Cambridge Acoustical Associates, Inc., Cambridge, Mass. Member AIAA.

†Professor, Department of Aeronautics and Astronautics. Associate Fellow AIAA.

vortex-induced upwash on the flight plane and, through superposition, the radiated acoustic pulse is then obtained. Such a theory will be an improved version of that developed by the authors in Ref. 6, wherein the basic two-dimensional, leading-edge loading solution originally derived by Adamczyk[1] and Amiet[2] was used in a simple spanwise superposition in order to model finite-span effects on acoustic radiation. The aerodynamic model in Ref. 6 did not accurately represent the strength and phase of acoustic sources near the blade tip.

From the acoustic viewpoint, the aerodynamic loading due to the blade passage through the gust represents a distribution of acoustic dipoles, each radiating a tone of the same frequency. At low speeds and/or for low gust-reduced frequencies, the tone's wavelength is much greater than the airfoil chord. The unsteady loading is then termed "acoustically compact"; for the acoustic calculation, it may be integrated over the chord to give the strength of a simple point acoustic dipole. When the ratio of wavelength to chord is not great, so that there are substantial differences in local values of the unsteady loading phase, the acoustic effect is not that of a single dipole. The pressure distribution itself, not its integrated value of unsteady sectional lift, must be used for the acoustic calculation. Such a loading is said to be acoustically noncompact.

The present model may be applied to physical situations in which the resulting aerodynamic loading may be anticipated to be largely noncompact, when the loading is expected to have high-level lift harmonics which can be calculated correctly only if compressibility and unsteady (noncompact) effects are properly taken into account. For helicopter blade/vortex interaction, the physical conditions which demand that a noncompact model be used to predict a substantial section of the loading spectrum are that the tip Mach number be close to 1, and/or that the vertical blade/vortex separation be small in comparison to the blade semichord. As discussed above, the trailing edge of the blade can then be neglected in the analysis for the unsteady loading. The present model, therefore, investigates a different operating regime from that studied by researchers who have developed aerodynamic models for blade/vortex interaction when the latter is assumed to be a low-speed, or largely low-frequency, (compact) phenomenon. It is intended to complement, for example, that of Chu,[7] who developed a numerical lifting-surface theory for a square-tip blade of semi-infinite span passing through a gust at $M=0$ and then applied it to calculate impulsive loads due to blade/vortex interaction.

The solution procedure used here to calculate the loading on the corner wing is an application of an idea by Carrier[8] for computing the temperature field of a heated corner plate; its main mathematical tool is the Wiener-Hopf technique. The solution we obtain is not exact because, as indicated below, we allow one of the boundary conditions in the complex boundary-value problem for the potential to be violated. However, we have shown in Ref. 9, Chap. 4 that the result thus obtained actually represents the first correction in an iterative source-cancellation scheme in which the inexactness of the answer becomes less and less significant. Landahl[10] has shown that the solution through iteration converges uniformly with respect to a parameter containing the gust-reduced frequency and the Mach number and that, for higher values of reduced frequency k_x or of Mach number M, fewer terms are needed to achieve a desired degree of accuracy. It follows that the loading obtained here should approach the exact one in the noncompact limit. Although the evaluation of the approximate result at all points on the plate is not practical here, since for each point the numerical evaluation of a complicated double integral is required, through an asymptotic analysis we are able to deduce the behavior of the loading away from the corner point and to corroborate quantitatively the implication of Landahl's convergence proof[10]: that the violation of the boundary condition does not appear to be great so long as the frequency is high and/or the Mach number close to 1.

The last step in the development is to use the conclusions of the asymptotic analysis to extract rationally from the calculated approximate solution a solution for the loading that does not violate the upstream boundary condition. This final simplified result is given in closed form and so may be applied readily to model the strength of acoustic dipoles near the tip of a helicopter blade passing over a vortex. It has the expected $\sqrt{y}$ behavior at the side edge and approaches the two-dimensional form[1-3] at spanwise points away from $y=0$. At the corner point itself, the predicted loading has a nonuniform behavior.

Formulation

Figure 1 shows the model; a rigid flat plate occupies the $0<x<\infty$, $0<y<\infty$ quadrant of the x-y plane and a freestream U $(M=U/c_0)$ convects the sinusoidal gust at interaction angle Λ. All distances are normalized by the wing semichord b, so that the position of the trailing edge for the actual wing may be indicated by a dotted line at $x=2$. The linear convected-wave equation governs the three-dimensional perturbation potential

$$\frac{\partial^2\Phi}{\partial x^2}+\frac{\partial^2\Phi}{\partial y^2}+\frac{\partial^2\Phi}{\partial z^2}-\frac{1}{c_0^2}\frac{D^2\Phi}{Dt^2}=0 \tag{1}$$

with boundary conditions

$$\Phi_z(x>0,y>0,0,t)=-w_0 b e^{i\omega t-ik_x x-ik_x \tan\Lambda y} \tag{2a}$$

$$\Phi(x,y<0,0,t)=\Phi(x<0,y,0,t)=0 \tag{2b}$$

where Eq. (2a) is the requirement of flow tangency and Eq. (2b) is due to the perturbation flow's antisymmetry about the $z=0$ plane, a characteristic of every planar lifting problem; ω is the gust's circular frequency; and $k_x=\omega b/U$, the chordwise gust wavenumber or reduced frequency. The three-dimensional pressure field P corresponding to Φ also satisfies the convected-wave operator of Eq. (1) and is also expected to have the following behavior at the edges:

$$P(x\to 0+,y>0,0,t)\sim 1/\sqrt{x} \tag{3a}$$

$$P(x>0,y\to 0+,0,t)\sim\sqrt{y} \tag{3b}$$

If we now let

$$y=Y/\sqrt{1-M^2} \tag{4a}$$

$$z=Z/\sqrt{1-M^2} \tag{4b}$$

$$\Phi=\phi_*\exp[i\omega t+k_x M^2 x/(1-M^2)] \tag{4c}$$

$$P=p_*\exp[i\omega t+k_x M^2 x/(1-M^2)] \tag{4d}$$

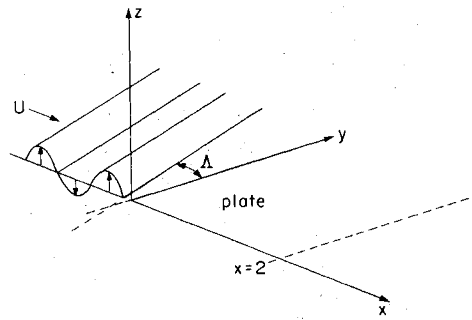

Fig. 1 The passage of a quarter-infinite flat-plate wing through an oblique gust.

we obtain the boundary-value problem for ϕ_*

$$\phi_{*xx}+\phi_{*YY}+\phi_{*ZZ}+K^2\phi_*=0 \tag{5}$$

subject to

$$\phi_{*Z}(x>0,Y>0,0)=-\frac{w_0 b}{\sqrt{1-M^2}}$$

$$\times\exp(-ik_x x/(1-M^2)-ik_x\tan\Lambda Y/\sqrt{1-M^2}) \tag{6a}$$

$$\phi_*(x<0,y,0)=\phi_*(x,y<0,0)=0 \tag{6b}$$

where $K=k_xM/(1-M^2)$. The relationship between ϕ_* and the pressure p_* is (Bernoulli's equation),

$$p_*=-\frac{\rho_0 U}{b}\left(\frac{ik_x}{1-M^2}+\frac{\partial}{\partial x}\right)\phi_* \tag{7}$$

Equations (5) and (6) cannot be solved in closed form by means of any simple analytical procedure known. The treatment which follows yields an approximate solution which should approach the exact one in the high-frequency limit; in order to obtain it, we allow the upstream condition $\phi_*(x<0,Y,0)=0$ to be violated for $Y>0$ by an amount later shown to be small for noncompact cases of interest.

Approximate Solution by the Wiener-Hopf Technique

We define the transform pair

$$\phi_*(x,Y,Z)=\int_{C_2}\frac{d\lambda_2}{\sqrt{2\pi}}e^{-i\lambda_2 Y}\int_{C_1}\frac{d\lambda_1}{\sqrt{2\pi}}e^{-i\lambda_1 x}\tilde{\phi}(\lambda_1,\lambda_2;Z) \tag{8a}$$

$$\tilde{\phi}(\lambda_1,\lambda_2;Z)=\iint_{-\infty}^{\infty}\frac{dx\,dY}{2\pi}e^{i\lambda_1 x+i\lambda_2 Y}\phi_*(x,Y,Z) \tag{8b}$$

where C_1 and C_2 denote complex integration contours in the λ_1 and λ_2 planes, respectively. If Eq. (8b) is applied to Eq. (5), the solution for positive Z is

$$\phi_*(x,Y,Z)=\int_{C_1}\frac{d\lambda_1}{\sqrt{2\pi}}e^{-i\lambda_1 x}$$

$$\times\int_{C_2}\frac{d\lambda_2}{\sqrt{2\pi}}e^{-i\lambda_2 Y-Z\sqrt{\lambda_1^2+\lambda_2^2-K^2}}\tilde{\phi}(\lambda_1,\lambda_2;0+) \tag{9}$$

Since $\phi_*(x,Y<0,0+)=0$, it follows from Eq. (9) with $Z=0+$ that $\tilde{\phi}(\lambda_1,\lambda_2;0+)$ must be an analytic function of λ_2 in the upper half of the λ_2 plane. Using the standard nomenclature of problems of the Wiener-Hopf type, we then write $\tilde{\phi}(\lambda_1,\lambda_2;0+)=\tilde{\phi}_\oplus$. From Eq. (9) the vertical velocity field $\partial\phi_*(x,Y,0)/\partial Z$, to cancel that of the gust on the plate's surface in order to satisfy flow tangency, may be calculated

$$\phi_{*Z}(x,Y,0+)=-\int_{C_1}\frac{d\lambda_1}{\sqrt{2\pi}}e^{-i\lambda_1 x}$$

$$\times\int_{C_2}\frac{d\lambda_2}{\sqrt{2\pi}}e^{-i\lambda_2 Y}\tilde{\phi}_\oplus(\lambda_1,\lambda_2;0+)\sqrt{\lambda_1^2+\lambda_2^2-K^2} \tag{10}$$

For simplicity of notation, throughout the analysis that follows $Z=0$ is understood to mean $Z=0+$. We now make the assumption which allows us to obtain an approximate solution to the boundary-value problem posed in Eqs. (5) and (6): the condition $\phi_*(x<0,y>0,0)=0$ is relaxed. We let

$$-\tilde{\phi}(\lambda_1,\lambda_2,0+)\sqrt{\lambda_1^2+\lambda_2^2-K^2}=\tilde{r}(\lambda_1,\lambda_2)+\tilde{v}(\lambda_1,\lambda_2) \tag{11}$$

where

$$r(x,Y)=0 \text{ for } Y<0, \quad =\text{2-D upwash for } Y>0 \tag{12a}$$

$$v(x,Y)=? \text{ for } Y<0, \quad =0 \text{ for } Y>0 \tag{12b}$$

In Ref. 3, the two-dimensional potential field for an infinite-span airfoil with no trailing edge passing through an oblique gust has been calculated [Eq. (12) there]:

$$\phi_*(x,Z)=\frac{ibw_0\exp(-ik_x\tan\Lambda Y/\sqrt{1-M^2})}{2\pi\sqrt{1-M^2}\sqrt{k_x/(1-M^2)+\mu}}\frac{Z}{|Z|}$$

$$\times\int_C\frac{d\lambda_1\exp\{-\sqrt{\lambda_1^2-\mu^2}\,|Z|-i\lambda_1 x\}}{\sqrt{\lambda_1-\mu}\,[\lambda_1-k_x/(1-M^2)]} \tag{13}$$

where the contour C_1 in the complex λ_1 passes over the pole at $\lambda_1=k_x/(1-M^2)$ and the branch point at $\lambda_1=\mu$. The frequency parameter μ is given by

$$\mu=\sqrt{\frac{k_x^2M^2}{(1-M^2)^2}-\frac{k_y^2}{1-M^2}}=\frac{k_x|\tan\Lambda|}{(1-M^2)}\left[\frac{M^2}{\sin^2\Lambda}-1\right]^{1/2}$$

From Eq. (13) the two-dimensional upwash field to be used in Eq. (11a) may be found,

$$r(x,Y)=\frac{-iw_0 b\exp(-ik_x\tan\Lambda Y/\sqrt{1-M^2})}{2\pi\sqrt{1-M^2}\sqrt{k_x/(1-M^2)+\mu}}$$

$$\times\int_{C_1}\frac{d\lambda_1 e^{-i\lambda_1 x}\sqrt{\lambda_1+\mu}}{[\lambda_1-k_x/(1-M^2)]} \tag{14}$$

so that

$$\tilde{r}(\lambda_1,\lambda_2)=\frac{A(\lambda_1)}{\lambda_2-k_x\tan\Lambda/\sqrt{1-M^2}} \tag{15}$$

where

$$A(\lambda_1)=\frac{w_0 b\sqrt{\lambda_1+\mu}}{2\pi\sqrt{1-M^2}\sqrt{k_x/(1-M^2)+\mu}}\,\frac{1}{[\lambda_1-k_x/(1-M^2)]} \tag{16}$$

In the solution being constructed, $\tilde{v}(x,Y>0)=0$ as stated in Eq. (12b). It follows, therefore, that $\tilde{v}(\lambda_1,\lambda_2)$ must be an analytic function of λ_2 over the lower half of the λ_2 plane, and so $\tilde{v}(\lambda_1,\lambda_2)=\tilde{v}_\ominus$. Substituting for $\tilde{r}$ and $\tilde{v}$ into Eq. (11), and factoring out the term $\sqrt{\lambda_1^2+\lambda_2^2-K^2}$,

$$-\tilde{\phi}_\oplus(\lambda_2)\sqrt{\lambda_2-(K^2-\lambda_1^2)^{1/2}}$$

$$=\frac{A(\lambda_1)}{\left[\lambda_2-\dfrac{k_x\tan\Lambda}{\sqrt{1-M^2}}\right]}\,\frac{1}{\sqrt{\lambda_2+(K^2-\lambda_1^2)^{1/2}}}$$

$$+\frac{\tilde{v}_\ominus(\lambda_2)}{\sqrt{\lambda_2+(K^2-\lambda_1^2)^{1/2}}} \tag{17}$$

where we write $\tilde{\phi}_\oplus(\lambda_2)$ instead of $\tilde{\phi}_\oplus(\lambda_1,\lambda_2)$ to avoid confusion as to the meaning of the symbol $\oplus$, which refers here to the analyticity of $\tilde{\phi}$ in the upper half of the λ_2 plane and not in the λ_1 plane.

Since an $\exp(i\omega t)$ behavior for the harmonic time dependence has been used, the condition of outward wave propagation, or Sommerfeld radiation condition, requires us to allow ω, and so also k_x and μ, to have a small negative imaginary part (Ref. 11, p. 28). In Eq. (17) the two radicals $\sqrt{\lambda_2-(K^2-\lambda_1^2)^{1/2}}$, and $\sqrt{\lambda_2+(K^2-\lambda_1^2)^{1/2}}$ contain the quantity $\sqrt{K^2-\lambda_1^2}$, a function of λ_1 which has branch points at $\lambda_1=\pm K$; the branch of $\sqrt{\lambda_1^2-K^2}$ with vanishing argument as $\lambda_1\to\infty$ along the C_1 contour is chosen. This choice now implies two new branch cuts in the λ_1 plane, which is then as shown in Fig. 2a. Figure 2b indicates the position of the singularities in the λ_2 plane and the corresponding regions of $\ominus$ and $\oplus$ analyticity.

If the first term on the right side of Eq. (17) is now split in the usual way into a sum of two functions, one $\oplus$ and the other $\ominus$, a Wiener-Hopf equation of the form $\oplus = \ominus$ is obtained from which $\tilde{\phi}_\oplus$ may be found in a straightforward manner after assuming that all functions satisfy the Riemann-Lebesgue lemma[12] and then invoking Liouville's theorem (Ref. 11, p. 6). The solution for $\tilde{\phi}_\oplus$ is

$$\tilde{\phi}_\oplus(\lambda_2) = \frac{-A(\lambda_1)}{\sqrt{\frac{k_x \tan\Lambda}{\sqrt{1-M^2}} + (K^2-\lambda_1^2)^{1/2}}} \frac{1}{\sqrt{\lambda_2 - (K^2-\lambda_1^2)^{1/2}}} \times \frac{1}{\left(\lambda_2 - \frac{k_x\tan\Lambda}{\sqrt{1-M^2}}\right)} \tag{18}$$

Substituting for A and using Eq. (9), we obtain $\phi_*(x,Y,Z)$. From the linearized relation between pressure and velocity potential [Eq. (7)], p_* may also be calculated. The final results are

$$\phi_*(x,Y,Z) = \frac{-w_0 b}{4\pi^2\sqrt{1-M^2}} \frac{1}{\sqrt{\frac{k_x}{1-M^2}+\mu}} \times \int_{C_1} \frac{d\lambda_1 e^{-i\lambda_1 x}\sqrt{\lambda_1+\mu}}{\left(\lambda_1 - \frac{k_x}{1-M^2}\right)\sqrt{\frac{k_x\tan\Lambda}{\sqrt{1-M^2}} + (K^2-\lambda_1^2)^{1/2}}} \times \int_{C_2} \frac{d\lambda_2 e^{-i\lambda_2 Y - Z\sqrt{\lambda_1^2+\lambda_2^2-K^2}}}{\left(\lambda_2 - \frac{k_x\tan\Lambda}{\sqrt{1-M^2}}\right)} \frac{1}{\sqrt{\lambda_2-(K^2-\lambda_1^2)^{1/2}}} \tag{19}$$

$$p_*(x,Y,Z) = -\frac{i\rho_0 w_0 U}{4\pi^2\sqrt{1-M^2}} \frac{1}{\sqrt{k_x/(1-M^2)+\mu}} \times \int_{C_1} \frac{d\lambda_1 e^{-i\lambda_1 x}\sqrt{\lambda_1+\mu}}{\sqrt{k_x\tan\Lambda/\sqrt{1-M^2}+(K^2-\lambda_1^2)^{1/2}}} \times \int_{C_2} \frac{d\lambda_2 e^{-i\lambda_2 Y - Z\sqrt{\lambda_1^2+\lambda_2^2-K^2}}}{(\lambda_2 - k_x\tan\Lambda/\sqrt{1-M^2})\sqrt{\lambda_2-(K^2-\lambda_1^2)^{1/2}}} \tag{20}$$

$\phi_*(x,Y<0,0) = p_*(x,Y<0,0) = 0$ since the λ_2 integrands are analytic in the upper halfs of their λ_2 planes. Letting $Z=0$ and evaluating the λ_2 in closed form for $Y>0$ by deforming the contour to the lower half λ_2 plane, the loading p_* is found:

$$p_*(x,Y>0,0+) = \frac{(i-1)\rho_0 w_0 U}{2\pi\sqrt{1-M^2}\sqrt{\frac{k_x}{1-M^2}+\mu}} \exp(-ik_x\tan\Lambda Y/\sqrt{1-M^2}) \times \int_{C_1} \frac{d\lambda_1 e^{-i\lambda_1 x}}{\sqrt{\lambda_1-\mu}} E\left[Y\left(\frac{k_x\tan\Lambda}{\sqrt{1-M^2}} - \sqrt{K^2-\lambda_1^2}\right)\right] \tag{21}$$

where $E(a)$ is the complex Fresnel integral of argument a defined by

$$E(a) = \int_0^a \frac{dt e^{it}}{\sqrt{2\pi t}}$$

which for small a behaves as $\sqrt{2/\pi}\,\sqrt{a}\exp(ia)$. Therefore, the solution for p_* in Eq. (21) has the expected $\sqrt{Y}$ behavior [Eq. (3b)].

In Ref. 9 we have rederived the loading given by Eq. (21) using the alternate method of source cancellations. The procedure uses a Green's function technique first developed by Schwartzschild[13] in his theoretical studies of electromagnetic diffraction, and then adapted by Landahl[4] to treat certain problems of unsteady transonic flow. This was also the method Amiet[2] used to calculate the loading on an infinite-span airfoil in subsonic flow passing through a gust. As previously discussed, Landahl[10] has shown that the source cancellation procedure converges uniformly with respect to $k_x/(1-M^2)$, so that fewer and fewer terms are needed to obtain an accurate answer as the gust-reduced frequency k_x is increased and/or as the Mach number M nears 1; therefore, the solution in Eq. (21), the first of the iterative cancellation solutions, should approach the true one on the wing for short gust wavelengths and/or for high flight speeds.

Asymptotic Behavior of Loading p_* Near Leading Edge

By construction, the integrand of the λ_2 integral is an analytic function of λ_2 in the upper half of the λ_2 plane and consequently $p_*(x,Y<0,0)=0$. However, the integrand of the λ_1 integral is not analytic everywhere in the upper half of the λ_1 plane and, as a result, the solution in Eq. (21) does not satisfy the condition $p_*(x<0,y>0,0)=0$; i.e., the loading is not zero on the part of the $Z=0$ plane ahead of the wing. The next step in the analysis is to determine how severely the result in Eq. (21) violates the upstream condition. In order to investigate the solution for small values of x (near the leading edge), we look at the large λ_1 asymptotic form of the integrand (at the same time Y not small). Expanding the Fresnel integral for large argument, then

$$p_*(x\to 0, Y>0;0) = -\frac{\rho_0 w_0 U}{2\pi\sqrt{1-M^2}} \frac{1}{\sqrt{\frac{k_x}{1-M^2}+\mu}} \times \Bigg\{ \exp[-ik_x\tan\Lambda Y/\sqrt{1-M^2}] \int_{C_1} \frac{d\lambda_1}{\sqrt{\lambda_1-\mu}} e^{-i\lambda_1 x} + \frac{e^{\pi i/4}}{\sqrt{\pi}\sqrt{Y}} \int_{C_1} \frac{d\lambda_1 e^{-i\lambda_1 x - Y\sqrt{K^2-\lambda_1^2}}}{\sqrt{\lambda_1-\mu}\left(\frac{k_x\tan\Lambda}{\sqrt{1-M^2}} - \sqrt{K^2-\lambda_1^2}\right)^{1/2}} + \frac{e^{\pi i/4}}{\sqrt{\pi}} \sum_{n=0}^{\infty} \frac{(-i)^{n+1}(2n+1)!}{Y^{n+3/2} n! 2^{2n+1}} \times \int_{C_1} \frac{d\lambda_1 e^{-i\lambda_1 x - Y\sqrt{K^2-\lambda_1^2}}}{\sqrt{\lambda_1-\mu}\left(\frac{k_x\tan\Lambda}{\sqrt{1-M^2}} - \sqrt{K^2-\lambda_1^2}\right)^{n+3/2}} \Bigg\} \tag{22}$$

The first term in the expansion [Eq. (22)] may be recognized from Ref. 3, Eq. (14) (with $Z=0$) as the two-dimensional solution $p_{*\text{2-D}}$ for loading on a leading-edge airfoil of infinite span. For completeness that result is reproduced here,

$$p_{*\text{2-D}}(x,Y,0+) = -\frac{\rho_0 w_0 U \exp(-i\pi/4 - i\mu x - ik_x\tan\Lambda Y/\sqrt{1-M^2})}{\sqrt{\pi}\sqrt{1-M^2}\sqrt{k_x/(1-M^2)+\mu}\,\sqrt{x}} \quad \text{for } x>0$$
$$= 0 \quad \text{for } x<0 \tag{23}$$

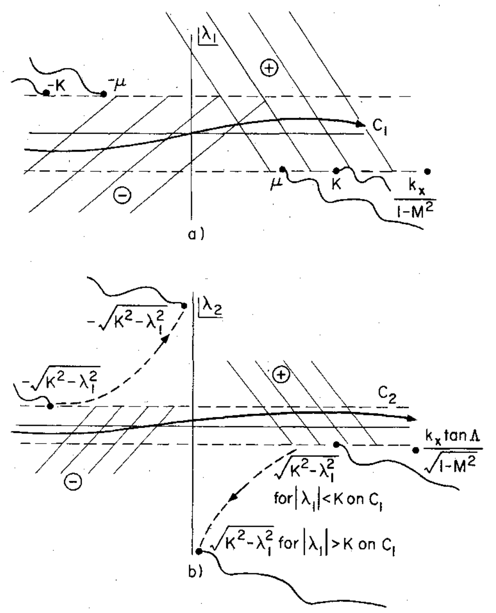

Fig. 2 Regions of ⊖ and ⊕ analyticity in the complex λ_1, λ_2 planes (integration contours C_1, C_2 are indicated).

Amiet[1] and Adamczyk[2] originally obtained the final result in Eq. (23) using alternate methods. We note that the leading contribution to the asymptotic behavior of the loading vanishes upstream, i.e., that the violation of the upstream boundary condition on p_* may be attributed to higher-order effects only. Since in Eq. (22) these contain a term of Y to a negative power, they represent a small correction as the distance $by = bY/\sqrt{1-M^2}$ from the edge ($Y=0$) is increased. The higher-order terms in Eq. (22) also contain complicated three-dimensional effects which should be larger as the corner is approached.

To calculate the coefficient of the $Y^{-1/2}$ term in Eq. (22), we must evaluate the integral I

$$I(x,Y>0) = \int_{C_1} \frac{d\lambda_1}{\sqrt{\lambda_1-\mu}} \exp[-i\lambda_1 x - Y\sqrt{\lambda_1^2-K^2}] \times \left\{ \frac{k_x \tan\Lambda}{\sqrt{1-M^2}} - \sqrt{K^2-\lambda_1^2} \right\}^{-1/2} \tag{24}$$

for $Y>0$, $x\to 0\pm$. Using the convolution theorem, we may rewrite it as

$$I(x,Y>0) = -i\sqrt{\frac{\pi}{2}} \int_{-\infty}^{\infty} d\xi H_1^{(2)}(K\sqrt{(x-\xi)^2+Y^2}) \times \frac{KY}{\sqrt{(X-\xi)^2+Y^2}} f(\xi) \tag{25}$$

where

$$f(\xi) = \int_{C_1} \frac{d\lambda_1}{\sqrt{2\pi}} \frac{e^{-i\lambda_1\xi}}{\sqrt{\lambda_1-\mu}} \frac{1}{\left(\dfrac{k_x \tan\Lambda}{\sqrt{1-M^2}} - \sqrt{K^2-\lambda_1^2}\right)^{1/2}} \tag{26}$$

The integrand in f has branch-point singularities at $\lambda_1 = \pm K$. Besides these, one finds that as $\lambda_1 \to \pm\mu$

$$\frac{1}{\left(\dfrac{k_x \tan\Lambda}{\sqrt{1-M^2}} - \sqrt{K^2-\lambda_1^2}\right)^{1/2}} \cong \left[\frac{2k_x \tan\Lambda}{\sqrt{1-M^2}}\right]^{1/2} \frac{1}{\sqrt{\lambda_1^2-\mu^2}}$$

so that it contains also a simple pole at $\lambda_1 = \mu$ and another branch point at $\lambda_1 = -\mu$. We write, therefore,

$$f(\xi) = f^{\pm\mu}(\xi) + f^{\pm K}(\xi) \tag{27}$$

$$I(x,Y) = I^{\pm\mu}(x,Y) + I^{\pm K}(x,Y) \tag{28}$$

where for large ξ, $f^{\pm\mu}(\xi)$ may be approximated by[14]

$$f^{\pm\mu}(\xi) = \frac{1}{\sqrt{2\pi}} \left[\frac{2k_x \tan\Lambda}{\sqrt{1-M^2}}\right]^{1/2} \int_{C_1} \frac{d\lambda_1 e^{-i\lambda_1\xi}}{(\lambda_1-\mu)\sqrt{\lambda_1+\mu}} \tag{29a}$$

If we take Eq. (29a) to hold for small ξ also, values of $f^{\pm\mu}(\xi)$ are overestimated; so that for $x<0$ the result thus obtained for $I^{\pm\mu}(x,Y)$ will represent a conservative estimate of the violation of the upstream boundary condition. The part $f^{\pm K}(\xi)$ is given by

$$f^{\pm K}(\xi) = \frac{1}{\sqrt{2\pi}} \int_{\substack{\text{Branch line} \\ \text{at } \lambda_1 = \pm K}} \frac{d\lambda_1 e^{-i\lambda_1\xi}}{\sqrt{\lambda_1-\mu}} \times \frac{1}{\left(\dfrac{k_x \tan\Lambda}{\sqrt{1-M^2}} - \sqrt{K^2-\lambda_1^2}\right)^{1/2}} \tag{29b}$$

The integrals $I^{\pm\mu}(x,Y)$, $I^{\pm K}(x,Y)$ in Eq. (28) in turn become

$$I^{\pm\mu}(x,Y) = -i\sqrt{\frac{\pi}{2}} \int_{-\infty}^{\infty} d\xi H_1^{(2)}(K\sqrt{(x-\xi)^2+Y^2}) \times \frac{KY}{\sqrt{(x-\xi)^2+Y^2}} f^{\pm\mu}(\xi) \tag{30a}$$

$$I^{\pm K}(x,Y) = -i\sqrt{\frac{\pi}{2}} \int_{-\infty}^{\infty} d\xi H_1^{(2)}(K\sqrt{(x-\xi)^2+Y^2}) \times \frac{KY}{\sqrt{(x-\xi)^2+Y^2}} f^{\pm K}(\xi) \tag{30b}$$

The function $f^{\pm\mu}(\xi)$ may now be calculated by deforming the contour C_1 in Fig. 3 to C_1^* or C_1^{**} for $x>0$ and $x<0$, respectively,

$$f^{\pm\mu}(\xi) = \frac{1}{\sqrt{2\pi}} \left[\frac{2k_x \tan\Lambda}{\sqrt{1-M^2}}\right]^{1/2} \frac{(-2\pi i)}{\sqrt{2\mu}} e^{-i\mu\xi}$$

$$\times \begin{cases} 1 & \text{for } \xi>0 \quad (31a) \\ 1-(1+i)E^*[2\mu(-\xi)] & \text{for } \xi<0 \quad (31b) \end{cases}$$

We have been able to calculate $f^{\pm\mu}(\xi)$ analytically. Unfortunately, the same cannot be done for the more complicated integrals in $f^{\pm K}(\xi)$, the contributions from the branch points at $\lambda_1 = \pm K$. However, these branch points are weak, so that their contribution to $f(\xi)$ for large ξ should be small in comparison to that from $f^{\pm\mu}(\xi\to\infty)$. The following approximation is then justified:

$$I^{\pm K}(x,Y) = -i\sqrt{\frac{\pi}{2}} \int_{-1/K}^{+1/K} d\xi H_1^{(2)}(K\sqrt{(x-\xi)^2+Y^2}) \times \frac{KY}{\sqrt{(x-\xi)^2+Y^2}} f^{\pm K}(\xi) \tag{32}$$

where $f^{\pm K}(\xi)$ may now be replaced by its small ξ behavior. The latter may be calculated by deforming C_1 to C_1^* and C_1^{**} in Fig. 4 for $x>0$ and $x<0$, respectively. The integrals that result turn out to be related to the well-known exponential integral, which for small argument (here $K\xi\to 0$) has the

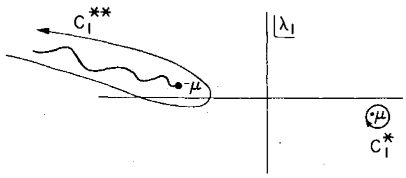

Fig. 3 Deformed contours C_1^*, C_1^{**} for $x>0$ and $x<0$, respectively.

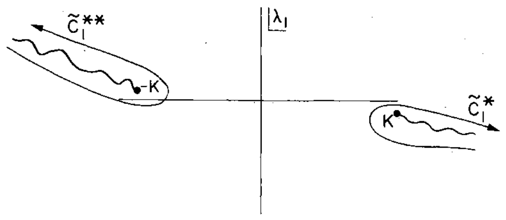

Fig. 4 Deformed contours $\tilde{C}_1^*$, $\tilde{C}_1^{**}$ for $x>0$ and $x<0$, respectively.

behavior given in Ref. 15. The final expressions for $f^{\pm K}(\xi)$ are

$$f^{\pm K}(\xi)=\frac{1}{\sqrt{\pi}}\begin{cases}=i[\gamma+\ln(iK\xi)-iK\xi] & \text{for } \xi>0 \quad \text{(33a)}\\ =\gamma+\ln(-iK(-\xi))-iK(-\xi) & \text{for } \xi<0 \quad \text{(33b)}\end{cases}$$

where γ is Euler's constant, approximately 0.577.

Since we are interested in small x and large Y behavior of $I^{\pm\mu}(x,Y)$, we may approximate the Hankel function in Eqs. (30) by its form for large argument. Equation (30a) then becomes

$$I^{\pm\mu}(x,Y)\cong\frac{K}{\sqrt{KY}}\exp(i\pi/4-iKY)\int_{-\infty}^{\infty}\mathrm{d}\xi e^{ikx\xi/Y}f^{\pm\mu}(\xi) \tag{34}$$

and similarly for $I^{\pm K}(x,Y)$, but with limits of integration $-1/K$ and $1/K$, so that the exponential may be further simplified to $\exp(iKx\xi/Y)=1+iKx\xi/Y$.

Performing the integrations for $I^{\pm\mu}$ and $I^{\pm K}$ and substituting the resulting expressions into Eq. (22), we obtain the first two terms in the asymptotic expansion of the loading near the leading edge

$$p_*(x\to 0,Y>0,0)=p_{*2\text{-D}}(x,Y,0)+\frac{(1+i)\exp(-iKY)}{\pi\sqrt{K}y\sqrt{1-M^2}}$$
$$\times\left\{1-\frac{\pi}{2}+i\gamma-\left(\frac{\gamma}{2}+\frac{i\pi}{4}-\frac{1}{4}\right)\frac{ix}{y\sqrt{1-M^2}}\right.$$
$$-(1+i)\pi\left(\frac{K}{\mu}\right)\left(\frac{k_x\tan\Lambda}{\sqrt{1-M^2}}\Big/\mu\right)^{1/2}\frac{1}{1-\dfrac{Kx}{\mu\sqrt{1-M^2}y}}$$
$$\left.\times\frac{1}{\sqrt{1+\dfrac{Kx}{\mu\sqrt{1-M^2}y}}}\right\} \tag{35}$$

Figure 5 is a plot of the magnitude of the second term on the right-hand side of Eq. (35), the leading-order three-dimensional correction to the two-dimensional loading near the leading edge. The values of M and Λ are 0.8 and 62 deg, so that $M_{\text{eff}}=M/\sin\Lambda=0.91$. For $b=0.3$ m (1 ft) and $\lambda_{\text{gust}}/b=2\pi\cos\Lambda/k_x=1/2$, the value of k_x is 5.9. Using the standard sound speed value of 335 m/s (1100 ft/s), the corresponding frequency $\omega/2\pi$ of the acoustic tone radiated

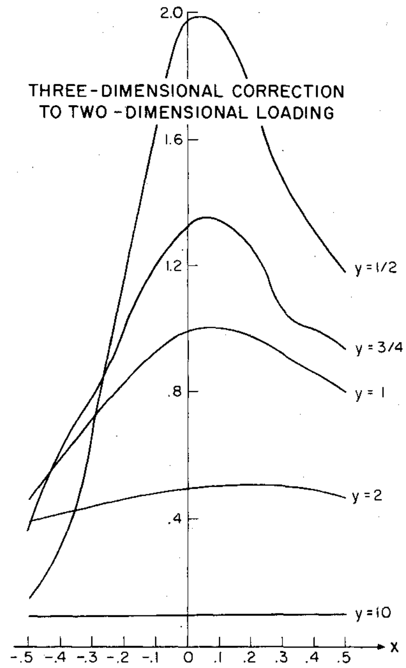

Fig. 5 Magnitude of second term in the asymptotic behavior of loading [Eq. (35)] near the leading edge.

due to such a wing/gust interaction would be 826 Hz. The figure shows that near the side edge ($y=1/2$) the first corrective contribution is larger on the plate side than upstream, indicating that the solution derived begins to predict three-dimensional effects on the plate side that are larger than the spurious behavior upstream. For larger values of y the correction flattens out until for $y=10$ it is practically a zero-slope line which, due to the algebraic decay with y away from the side edge, contains loading correction values about 5% of those for $y=1/2$.

Solution for p_* Satisfying the Upstream Condition

For $Z=0$ the integrand of the λ_2 transform in Eq. (20) is composed of two parts: 1) a pole at $\lambda_2=k_x\tan\Lambda/\sqrt{1-M^2}$ and 2) a branch line singularity at $\lambda_2=\sqrt{K^2-\lambda_1^2}$. For large Y, the pole gives the loading the simple sinusoidal $\exp(-ik_x\tan\Lambda Y/\sqrt{1-M^2})$ spanwise variation of the input gust or of the loading on an infinite-span wing.[1-3] It follows, therefore, that the branch line must account for the three-dimensional effects in the solution and thus allow the latter to satisfy the side-edge condition of $p_*(x,Y\to 0+,0)\cong\sqrt{Y}$. As shown in the analysis below, the branch line also implies a phase variation for the loading near the tip very different from that of the input gust.

The integrand in Eq. (20) indicates that the effects of the leading and side edges are coupled, for it cannot be factored into a product of a function of λ_1 and another of λ_2, and so the λ_1 and λ_2 integrations cannot be performed separately. The analysis to follow is intended to study in more detail the x-Y coupling and to extract rationally a simplified lifting-surface theory which satisfies the upstream boundary condition; it reveals that at high frequencies the coupling is essentially limited in importance to the corner point itself: the simplified result derived in this section satisfies the upstream boundary condition and does not have x-Y coupling; as a penalty, however, it exhibits a nonuniform behavior at $x=0$, $Y=0$.

The integral in Eq. (21) may be re-expressed as

$$(1-i)\int_0^{\infty}\frac{\mathrm{d}\xi}{\sqrt{\xi}}e^{-i\mu\xi}g(x-\xi) \tag{36}$$

where

$$g(x)=\int_{-\infty}^{\infty}\frac{\mathrm{d}\lambda}{\sqrt{2\pi}}\,e^{-i\lambda x}E\left[Y\left(\frac{k_x\tan\Lambda}{\sqrt{1-M^2}}-\sqrt{K^2-\lambda^2}\right)\right] \quad (37)$$

We now split the integral in Eq. (37) into three segments, as indicated by Eq. (38) and then for each segment interchange orders of integration with the Fresnel integral. The results are given in Eq. (39).

$$\sqrt{2\pi}g(x)=\int_{-\infty}^{-K}+\int_{-K}^{K}+\int_{K}^{\infty} \quad (38)$$

1) $2\pi\delta(x)E\left[Y\left(\frac{k_x\tan\Lambda}{\sqrt{1-M^2}}-K\right)\right]$

2) $+-2\frac{\sin Kx}{x}\left\{E\left[Y\frac{k_x\tan\Lambda}{\sqrt{1-M^2}}\right]-E\left[Y\left(\frac{k_x\tan\Lambda}{\sqrt{1-M^2}}-K\right)\right]\right\}$

3) $+2\pi\delta(x)\int_{Y[k_x\tan\Lambda/(1-M^2)^{1/2}]}^{Y[k_x\tan\Lambda/(1-M^2)^{1/2}]+i\infty}\frac{\mathrm{d}te^{it}}{\sqrt{2\pi t}}$

4) $+\int_{Y\{k_x\tan\Lambda/(1-M^2)^{1/2}-K\}}^{Y[k_x\tan\Lambda/(1-M^2)^{1/2}]}\frac{\mathrm{d}te^{it}}{\sqrt{2\pi t}}$

$\times\int_{-(K^2-\{(t/Y)-k_x\tan\Lambda/(1-M^2)^{1/2}\}^2)^{1/2}}^{+(K^2-\{(t/Y)-k_x\tan\Lambda/(1-M^2)^{1/2}\}^2)^{1/2}}\mathrm{d}\lambda e^{-i\lambda x}$

5) $-\int_{Y[k_x\tan\Lambda/(1-M^2)^{1/2}]}^{Y[k_x\tan\Lambda/(1-M^2)^{1/2}]+i\infty}\frac{\mathrm{d}te^{it}}{\sqrt{2\pi t}}$

$\times\int_{-(K^2-\{(t/Y)-k_x\tan\Lambda/(1-M^2)^{1/2}\}^2)^{1/2}}^{+(K^2-\{(t/Y)-k_x\tan\Lambda/(1-M^2)^{1/2}\}^2)^{1/2}}\mathrm{d}\lambda e^{-i\lambda x} \quad (39)$

where certain terms have been grouped and numbered for convenience in the discussion that follows. Only integrals 4 and 5 contain x-Y coupling; all others involve products of a function of x and another of Y.

Since $E(\infty)=(1+i)/2$, a constant, for large Y terms integrals 2-5 vanish; only integral 1 remains. For $Y\to 0+$, integrals 3 and 5 may be deformed in the complex t plane from the positive real axis to the positive imaginary axis. Respectively, they become

$$e^{i\pi/4}\int_0^{\infty}\frac{\mathrm{d}\xi e^{-\xi}}{\sqrt{2\pi\xi}}\cdot 2\pi\delta(x) \quad (40)$$

$$-e^{i\pi/4}\int_0^{\infty}\frac{\mathrm{d}\xi e^{-\xi}}{\sqrt{2\pi\xi}}\int_{-(K^2+\xi^2/Y^2)^{1/2}}^{(K^2+\xi^2/Y^2)^{1/2}}\mathrm{d}\lambda e^{-i\lambda x} \quad (41)$$

For $Y\to 0+$, the inside integral in Eq. (41) gives $2\pi\delta(x)$, so that the first-order contribution of integrals 3 plus 5 is zero. Higher-order contributions vanish as well.

In order to obtain the behavior of integral for 4 $Y\to 0+$, we integrate by parts

$$\lim_{Y\to 0+}(4)\cong\sqrt{\frac{2}{\pi}}\sqrt{t}e^{it}\int_{-(K^2-\{(t/Y)-k_x\tan\Lambda/(1-M^2)^{1/2}\}^2)^{1/2}}^{+(K^2-\{(t/Y)-k_x\tan\Lambda/(1-M^2)^{1/2}\}^2)^{1/2}}\mathrm{d}\lambda e^{-i\lambda x}$$

$$\times\Big|_{t=Y\{[k_x\tan\Lambda/(1-M^2)^{1/2}]-K\}}^{t=Y[k_x\tan\Lambda/(1-M^2)^{1/2}]}=\frac{2\sin Kx}{x}$$

$$\times\sqrt{\frac{2}{\pi}}\sqrt{\frac{k_x\tan\Lambda Y}{(1-M^2)^{1/2}}}\exp\left(\frac{ik_x\tan\Lambda Y}{\sqrt{1-M^2}}\right) \quad (42)$$

which may be interpreted as the small Y behavior of

$$\lim_{Y\to 0+}(4)=\frac{2\sin Kx}{x}E\left[Y\frac{k_x\tan\Lambda}{\sqrt{1-M^2}}\right] \quad (43)$$

So that near the side edge integral 4 cancels the first term of integral 2. The sum of all terms in Eq. (39) for $Y\to 0+$ is therefore

$$\sqrt{2\pi}g(x)\simeq\left\{2\pi\delta(x)+\frac{2\sin Kx}{x}\right\}E\left[Y\left(\frac{k_x\tan\Lambda}{\sqrt{1-M^2}}-K\right)\right] \quad (44)$$

from which

$$\sqrt{2\pi}g(x-\xi)\cong\left\{2\pi\delta(x-\xi)\right.$$

$$\left.+\frac{2\sin[K(x-\xi)]}{x-\xi}\right\}E\left[Y\left(\frac{k_x\tan\Lambda}{\sqrt{1-M^2}}-K\right)\right] \quad (45)$$

In the convolution, Eq. (36), the second term in brackets in Eq. (45) makes a contribution which is nonzero for $x<0$, but which is, however, well behaved and finite valued. Therefore, it may be neglected in comparison to the δ function term which contributes $1/\sqrt{x}$ for $x>0$ and zero for $x<0$, a much more important part of the blade's acoustic source strength due to its singular behavior at $x=0+$. Evaluating the convolution, then, we obtain, with $y=Y/\sqrt{1-M^2}$, the simplified lifting-surface result for a quarter-infinite wing passing through a gust at high subsonic speed,

$$p_*(x,Y>0,0)=i\sqrt{\frac{2}{\pi}}\frac{\rho_0 w_0 U}{\sqrt{1-M^2}}\frac{1}{\sqrt{\frac{k_x}{1-M^2}+\mu}}$$

$$\times\frac{1}{\sqrt{x}}E\left[k_x y\left(\tan\Lambda-\frac{M}{\sqrt{1-M^2}}\right)\right]\exp(-i\mu x-ik_x\tan\Lambda y) \quad (46)$$

which for small y becomes

$$p_*(x,y\to 0+,0)\simeq i\frac{2}{\pi}\frac{\rho_0 w_0 U}{\sqrt{1-M^2}}\frac{1}{\sqrt{\frac{k_x}{\sqrt{1-M^2}}+\mu}}\frac{1}{\sqrt{x}}$$

$$\times\exp(-i\mu x-iKy\sqrt{1-M^2})\cdot\sqrt{k_x}(\tan\Lambda-M/\sqrt{1-M^2})^{1/2}\sqrt{y} \quad (47)$$

so that the corner point $x=0$, $Y=0$ is point of nonuniformity. The y variation of the loading phase near the side is therefore $\exp(-iKy\sqrt{1-M^2})$ rather than $\exp(-ik_x y\tan\Lambda)$, the spanwise phase variation for the input gust, and for the loading $p_{*2\text{-D}}$ far from the side edge. Since the loading's rate of decay as $y\to 0+$ is given by the constant

$$(k_x\tan\Lambda/\sqrt{1-M^2}-K)^{1/2}$$
$$=\sqrt{k_x}(\tan\Lambda-M/\sqrt{1-M^2})^{1/2}/(1-M^2)^{1/4}$$

which could be $\gg\sqrt{K}\sqrt{1-M^2}$ for the large Λ wing/gust interactions considered here, we conclude that the spanwise variation of the loading phase is small throughout the "tip region."

For large y (far from the side edge), Eq. (46) becomes Eq. (23), the expression for $p_{*2\text{-D}}$. Figure 6 is a plot of the magnitude of $\sqrt{2}$ times the Fresnel integral term in Eq. (46), the spanwise part of the derived pressure distribution which appears multiplying $p_{*2\text{-D}}$ given by Eq. (23). The $\sqrt{y}$ behavior for $y=0$ is indicated, as well as the asymptotic approach to 1 for large y [so that $p_*\to p_{*2\text{-D}}$ in Eq. (46)].

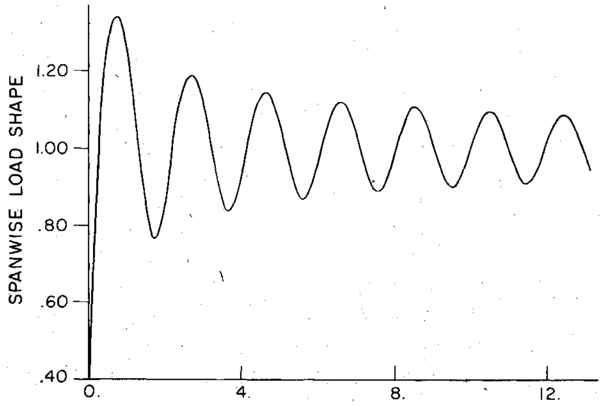

Fig. 6 Magnitude of $\sqrt{2}$ times Fresnel integral term in Eq. (46).

Finally, since the loading in Eq. (46) shows no x-y coupling (i.e., it is a simple product of a function of x and another of y), a trailing-edge correction may be performed to yield the loading on a square-tip blade, with finite chord and semi-infinite span, passing at high speed through a gust. The procedure to accomplish this has been discussed in detail in Refs. 1-3 and will not be repeated here. The result is

$$p_*(x>0,Y>0,0)=i\sqrt{\frac{2}{\pi}}\frac{1}{\sqrt{1-M^2}}\frac{\rho_0 w_0 U}{\sqrt{\frac{k_x}{1-M^2}+\mu}}\exp(-i\mu x$$

$$-ik_x\tan\Lambda y)\left\{\frac{1}{\sqrt{x}}-\frac{1}{\sqrt{2}}[1-(1+i)E^*[2\mu(2-x)]]\right\}$$

$$\times E\left[k_x y\left(\tan\Lambda-\frac{M}{\sqrt{1-M^2}}\right)\right] \tag{48}$$

Summary and Conclusions

An approximate solution has been obtained for the unsteady loading near the square tip of a semi-infinite-span wing passing through an oblique gust. The model assumes that either the gust wavelength is short in comparison to the wing semichord or that the subsonic flight Mach number is close to 1. The loading solution obtained is not exact, because the upstream boundary condition was relaxed during the solution process to make the problem treatable analytically by the technique applied: that of Wiener-Hopf. However, for noncompact cases, this departure from the correct theoretical result should be small. The authors[9] have shown, in fact, that the solution in Eq. (21) may be derived alternately using an iterative source cancellation technique which has been proved[10] to converge uniformly as a function of a physical parameter given by the gust-reduced frequency k_x divided by $1-M^2$. Therefore, the solution for the loading given here in Eq. (21) should approach the exact one in the limits $k_x \to \infty$ and/or $M \to 1$.

The basic result obtained [Eq. (21)] was analyzed further to extract rationally a simplified form [Eq. (46)] which satisfied the upstream condition earlier violated. This new result is also approximate, however, and our main purpose in deriving it was to develop a simple model for the strength of acoustic dipoles near the square tip of a helicopter blade passing over a vortex. The oblique gust in the present model can then be used as a Fourier component of the vortex-induced upwash on the rotor plane and, upon summation of their individual effects (acoustic tones), the theoretical far-field pulse may be calculated.

We found that the predicted loading near the tip has a phase variation which could be much smaller for large interaction angle Λ than that of the input gust. Physically, the resulting far-field pattern of reinforcement and cancellation of dipole sources may be expected to differ, perhaps substantially, from that obtained using a spanwise loading which matches the gust in phase variation and should be the subject of future acoustic studies.

Acknowledgment

This work was supported by NASA Grant NSG-2142.

References

[1] Adamczyk, J. J., "The Passage of an Infinite-Swept Airfoil through an Oblique Gust," NASA CR-2395, May 1974.

[2] Amiet, R. K., "High-Frequency Thin Airfoil Theory for Subsonic Flow," *AIAA Journal*, Vol. 14, Aug. 1976, pp. 1076-1082.

[3] Martinez, R. and Widnall, S. E., "Unified Aerodynamic-Acoustic Theory for a Thin Rectangular Wing Encountering a Gust," *AIAA Journal*, Vol. 18, June 1980, pp. 636-645.

[4] Landahl, M. T., *Unsteady Transonic Flow*, Pergamon Press, New York, 1961, Chap. 6, pp. 63-73.

[5] Miles, J. W., "The Oscillating Rectangular Airfoil at Supersonic Speeds," *Quarterly Journal of Applied Mathematics*, Vol. 9, No. 1, 1951, pp. 47-65.

[6] Martinez, R. and Widnall, S. E., "An Aeroacoustic Model for High-Speed, Unsteady Blade-Vortex Interaction," *AIAA Journal*, to be published.

[7] Chu, S. and Widnall, S. E., "Lifting-Surface Theory for a Semi-Infinite Wing in Oblique Gust," *AIAA Journal*, Vol. 12, Dec. 1974, pp. 1672-1678.

[8] Carrier, G. F., "Analytic Approximation Techniques in Applied Mathematics," *SIAM*, Vol. 13, March 1965, pp. 91-95.

[9] Martinez, R. and Widnall, S. E., "Aeroacoustic Theory for Noncompact Wing-Gust Interaction," MIT Fluid Dynamics Research Laboratory, Rept. 81-7, Oct. 1981, Chap. 4, pp. 69-71.

[10] Landahl, M. T., "Theoretical Studies of Unsteady Transonic Flow-IV. The Oscillating Rectangular Wing with Control Surface," Aeronautical Research Institute of Sweden (FFA), Rept. 80, 1958.

[11] Noble, B., "Methods Based on the Wiener-Hopf Technique," *International Series of Monographs on Pure and Applied Mathematics*, Pergamon Press, New York, 1958, pp. 6, 28.

[12] Carslaw, H. S., *An Introduction to the Theory of Fourier's Series and Integrals*, Dover, New York, 1950, p. 271.

[13] Schwartzschild, K., "Die Beugung und Polarisation des Lichts durch einen Spalt-I," *Mathematische Annalen*, Vol. 55, 1902, pp. 177-247.

[14] Carrier, G. F., Krook, M., and Pearson, C. E., *Functions of a Complex Variable, Theory and Technique*, McGraw Hill Book Co., New York, 1966, p. 256.

[15] Bender, C. M. and Orszag, S. A., *Advanced Mathematical Methods for Scientists and Engineers*, McGraw Hill Book Co., New York, 1978, pp. 251-252.